

Project	IEEE 802.16 Broadband Wireless Access Working Group < http://ieee802.org/16 >	
Title	Symmetric UL/DL diversity permutations for OFDMA PHY	
Date Submitted	2005-1-11	
Source(s)	Ran Yaniv, Tal Kaitz, Vladimir Yanover, Naftali Chayat Alvarion Ltd. Yuval Lomnitz Intel Dave Pechner, Todd Chauvin, Doug C. Dahlby ArrayComm Bin-Chul Ihm, Yongseok Jin, Jinyoung Chun, Kyuhyuk Chung LG Electronics, Inc.	ran.yaniv@alvarion.com tal.kaitz@alvarion.com yuval.lomnitz@intel.com dpechner@arraycomm.com chauvin@arraycomm.com dahlby@arraycomm.com bcihm@lge.com jayjay@lge.com jychun03@lge.com kyuhyuk@lge.com
Re:	Call for contributions, IEEE P802.16e/D5 Sponsor Ballot	
Abstract		
Purpose		
Notice	This document has been prepared to assist IEEE 802.16. It is offered as a basis for discussion and is not binding on the contributing individual(s) or organization(s). The material in this document is subject to change in form and content after further study. The contributor(s) reserve(s) the right to add, amend or withdraw material contained herein.	
Release	The contributor grants a free, irrevocable license to the IEEE to incorporate material contained in this contribution, and any modifications thereof, in the creation of an IEEE Standards publication; to copyright in the IEEE's name any IEEE Standards publication even though it may include portions of this contribution; and at the IEEE's sole discretion to permit others to reproduce in whole or in part the resulting IEEE Standards publication. The contributor also acknowledges and accepts that this contribution may be made public by IEEE 802.16.	
Patent Policy and Procedures	The contributor is familiar with the IEEE 802.16 Patent Policy and Procedures < http://ieee802.org/16/ipr/patents/policy.html >, including the statement "IEEE standards may include the known use of patent(s), including patent applications, provided the IEEE receives assurance from the patent holder or applicant with respect to patents essential for compliance with both mandatory and optional portions of the standard." Early disclosure to the Working Group of patent information that might be relevant to the standard is essential to reduce the possibility for delays in the development process and increase the likelihood that the draft publication will be approved for publication. Please notify the Chair < mailto:chair@wirelessman.org > as early as possible, in written or electronic form, if patented technology (or technology under patent application) might be incorporated into a draft standard being developed within the IEEE 802.16 Working Group. The Chair will disclose this notification via the IEEE 802.16 web site < http://ieee802.org/16/ipr/patents/notices >.	

Symmetric UL/DL diversity permutations for OFDMA PHY

Ran Yaniv, Tal Kaitz, Naftali Chayat, Vladimir Yanover
Alvarion Ltd.

1 Introduction

The objective of this contribution is to introduce downlink permutation schemes that are symmetric to the uplink PUSC permutation schemes currently defined. The motivation is to enable optimal adaptive beamforming through pairing of UL and DL allocations while maintaining the desired properties of uplink PUSC structures, namely frequency diversity and cell-based tile permutations.

The contribution is organized as follows. The problem is stated in the next section, followed by an outline of the proposed solution. Detailed text changes are presented in section 4.

2 Problem Statement

Permutations in which subcarriers are adjacent or piecewise-adjacent are particularly useful for AAS use, because the continuity in the frequency domain allows for improved channel estimation, a critical feature for AAS operation. AMC and the tile structures that exist in [6] (such as the uplink PUSC and optional PUSC) are examples of such structures.

AMC transmissions occur, by design, over a *single* contiguous frequency band and thus provide no frequency diversity. This feature allows the MAC layer to select, for each SS, the optimal frequency band for operation. This scheme was shown to provide a significant performance advantage. However for this scheme to operate, the channel needs to remain relatively static over periods of time equivalent to the MAC layer latency and processing time. In medium to high vehicular velocities, the MAC layer will not accommodate the fast channel variations.

It can be argued that other modes, such as the downlink PUSC and FUSC modes provide ample frequency diversity. However, these modes are less suitable for AAS operation since training signals are shared among all the subchannels. As a consequence, beamforming cannot be done separately for each subchannel, but rather for each major group in downlink PUSC mode, and over the entire bandwidth in FUSC mode.

Another argument that can be made is that spatial diversity, typically provided in AAS systems, compensates for the lack of frequency diversity. In the next subsection it is shown that even when spatial diversity is present, frequency diversity can significantly reduce the required fade margin.

The solution we propose contains more pilot overhead compared to other downlink structures that are defined [6]. These additional pilots are especially important in a mobile AAS environment, where the AAS preambles are of limited use due to large channel variations over time.

2.1 The importance of frequency diversity

In this section we analyze interaction of frequency diversity and spatial diversity. In the following we shall use the notation suggested in [4]. Consider the system described in Figure 1. The BS is located at the origin of the coordinate system. The BS consists of two antennas located at $x=\pm d/2$. The SS is located at a distance D from the BS. The line joining the SS with the BS makes an angle Φ_0 with the x -axis. The SS is surrounded by a scattering region of radius σ_s . A precise definition of σ_s will be provided later on. Note that σ_s is not restricted to be smaller than D , and the scattering region may encompass the BS.

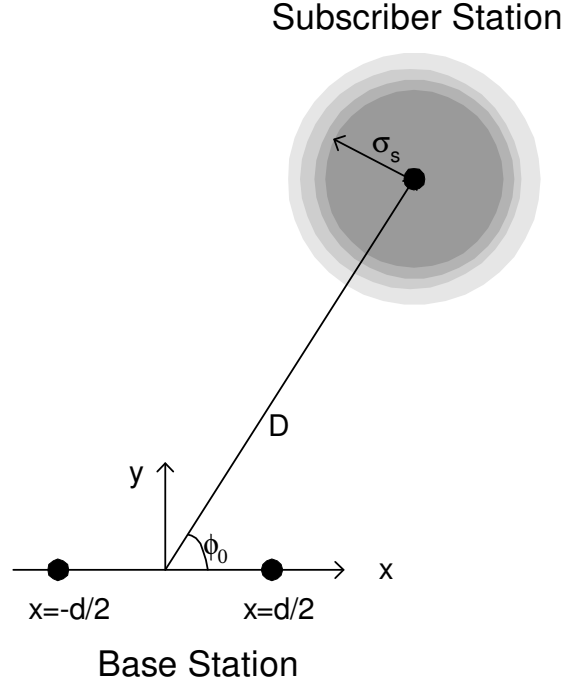


Figure 1 System model

Let $P_{AS}(\Phi)$ denote the power azimuth spectrum associated with the scattering region. The correlation between the signals received at base station antennas is given by

$$\rho_s(d) = \int \exp(jkd \cos \phi) P_{AS}(\phi) d\phi \quad (1)$$

where $k = 2\pi/\lambda$ and λ is the wavelength of the RF carrier.

Let $P_{DS}(\tau)$ denote the delay spread spectrum associated with the scattering region. The correlation between the signal received at frequencies f_1 and f_2 is given by

$$\rho_f(\Delta f) = \frac{1}{2\pi} \int \exp(j2\pi\Delta f \cdot \tau) P_{DS}(\tau) d\tau \quad (2)$$

with $\Delta f = f_1 - f_2$.

Next we make use of a Geometrically Based Single-Bounce (GBSB) statistical channel modeling approach (see [1] for an overview of spatial channel models) where the propagation between the SS and the BS are assumed to take place via single scattering from obstacles in the scattering region. This region is characterized by the probability density function of the scattering obstacles.

In particular we make use of a Gaussian Scattering Model (GSM). The GSM was proposed in [2] and [3]. The obstacle probability density of the GSM is given by

$$p(x_m, y_m) = \frac{1}{2\pi\sigma_s^2} \exp\left(-\frac{x_m^2 + y_m^2}{2\sigma_s^2}\right) \quad (3)$$

Here, x_m and y_m denote the coordinate of the obstacle relative to the SS.

In [4], Janaswamy derived closed form expressions for the power azimuth spectrum (PAS) and the power delay spread spectrum (PDS) for the GSM. Using expressions for PAS and PDS, he showed agreement to the measurement results provided by Pedersen, [5].

Although close form analytical expressions exist, we have used Monte Carlo techniques to compute the spatial and frequency correlations given in (1) and (2). We used the following conditions

- Carrier frequency $f_{RF} = 2.6\text{GHz}$
- Frequency separation $\Delta f = 5/6\text{ MHz}$.
- Spatial separation $d = 10\lambda$.
- 30 obstacles were generated fro each simulation round, 10000 simulation rounds were performed.

The value of D was varied in the range of 100m to 4km. The value of σ_s was varied from 10m to 200m. (For reference, the values found by Pederson corresponded to $D = 1.5\text{Km}$, $\sigma_s = 162\text{m}$)

The results are shown in Figure 2 where the spatial (solid lines) and frequency (dashed lines) correlation are shown. As can be seen, for large distances, the frequency correlation depends mostly on the scattering radius. The spatial correlation depends both on the scattering radius and BS-SS distance. (Actually it depends on the ratio of the two).

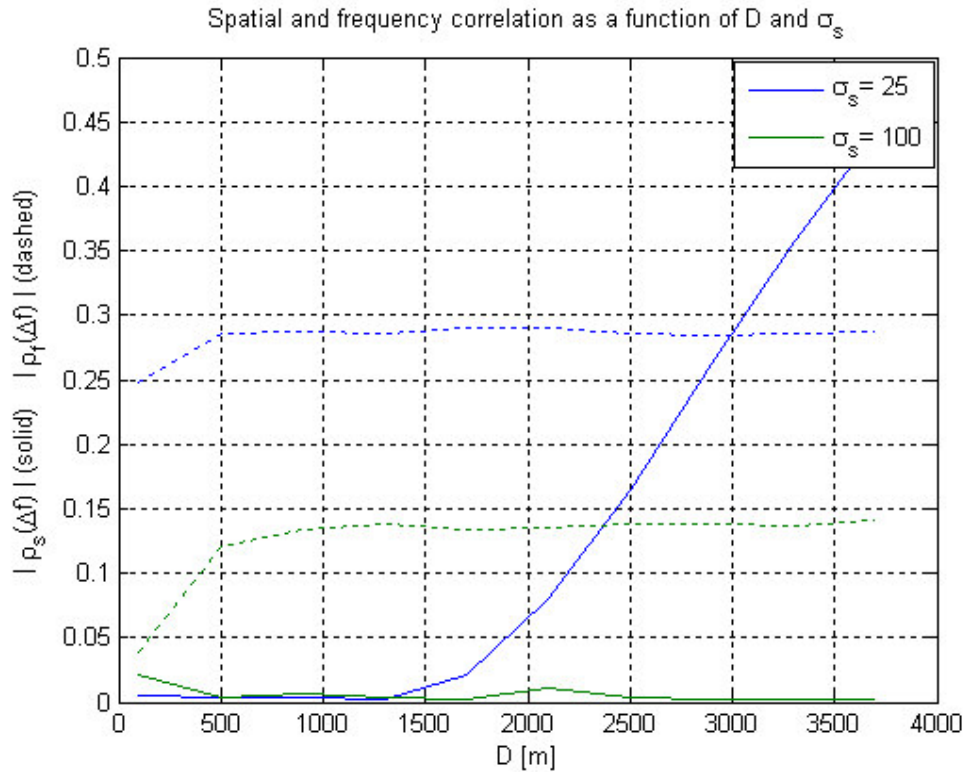


Figure 2 Spatial and frequency correlation

For large scattering radius, both correlations are low. As the scattering radius is reduced, both spatial and frequency correlations increase. For large angular spreads, (i.e. large ratios of σ_s/D), spatial correlation is lower than the frequency correlation. However for small angular spreads, frequency correlation is smaller. For the lowest angular spreads simulated, the antennas became completely correlated.

As a general conclusion, it seems that frequency diversity is important for macro-cell environment, where the distances are high and the angular spreads are small. For the microcell and picocell environments, where the angular spreads are high, spatial diversity is more important.

To evaluate the impact on system performance, we look at the required fade margin for a 1% outage probability, for the case of $\sigma_s=25$ m. The fade margin is computed for the case of four antennas ($d=10$) and 6 frequencies ($\Delta f=5/6$ MHz). The results are shown in Figure 3. For this simulation, 50000 trials were run.

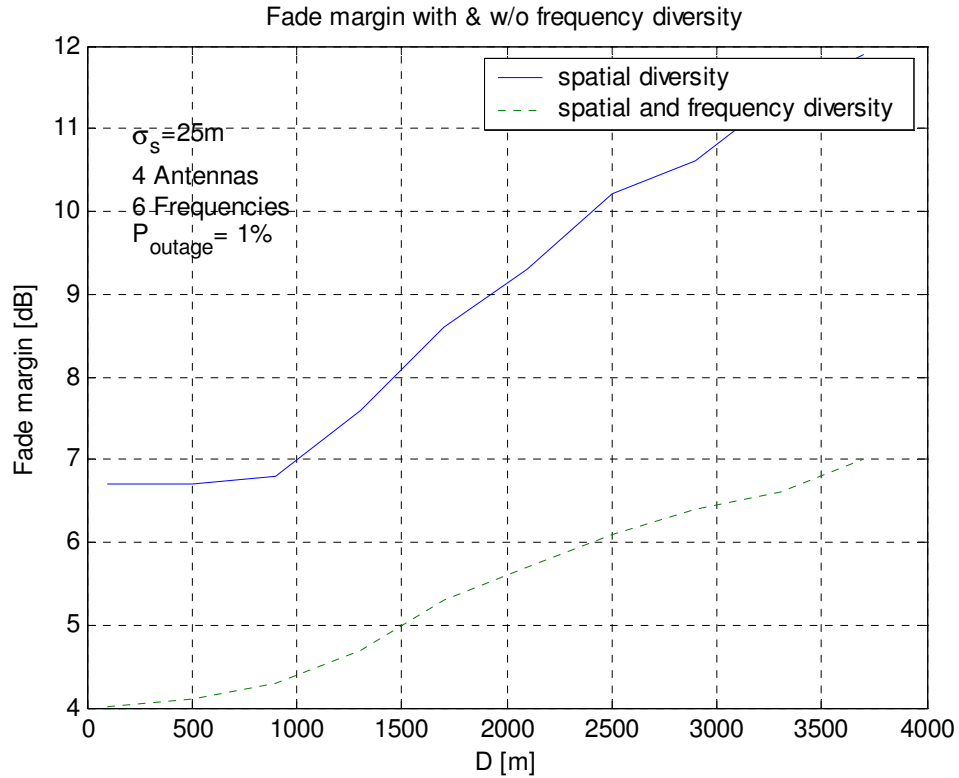
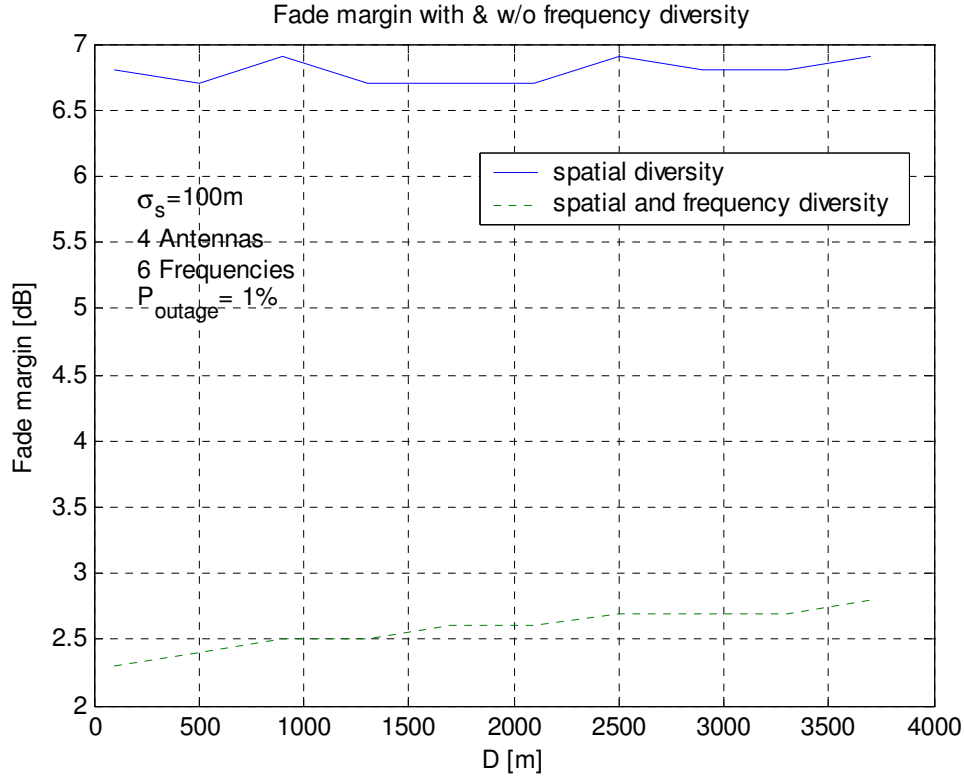


Figure 3 Fade margin

In the case of high angular spreads (low D), frequency diversity provides a reduction in fade margin of 2.5-3dB. In this case the antennas are uncorrelated, and frequency diversity increases diversity order to about 24. When D is increased the antennas become more correlated but the response across frequencies remains uncorrelated. The effective diversity order is reduced to an order of 6. In this case the improvement in fade margin is about 5dB.

Finally we look at the case of $\sigma_s=100\text{m}$. The antenna spacing and frequency spacing remain the same (10λ and $\Delta f=5/6\text{MHz}$ respectively). In this case, the spatial correlation remains low even at high D. Nevertheless, the improvement in diversity due to frequency diversity is about 4 dB.



2.2 Fade Margin

In order to gain some additional insight and to provide further validation for the results of the previous section, we now calculate the fade margin for a given outage probability and for several diversity orders.

Consider a system receiving N uncorrelated signals $x_i(t)$, $i=1..N$, with total mean power of P_{ave} . The signals may originate from multiple uncorrelated antenna elements and/or from uncorrelated frequency bands. The instantaneous power of the combined received signal $y(t)$ is

$$P = |y(t)|^2 = \sum_{i=1}^N |x_i(t)|^2 \quad (4)$$

For $x_i(t)$ that are Gaussian complex i.i.d., the distribution of P is χ^2 with $2N$ degrees of freedom, and the outage probability vs. fade margin can be readily obtained from the CDF of P .

Let us now examine the AMC and the uplink-PUSC permutations. A system employing the AMC permutation with M antenna elements spaced 10λ apart achieves a diversity order of M , while a system employing the UL PUSC diversity permutation with the same antenna array achieves a diversity order of $6M$, assuming that the correlation between frequencies spaced $BW/6$ apart is sufficiently low.

The following figure shows the outage probability vs. fade margin for several values of M with both permutations.

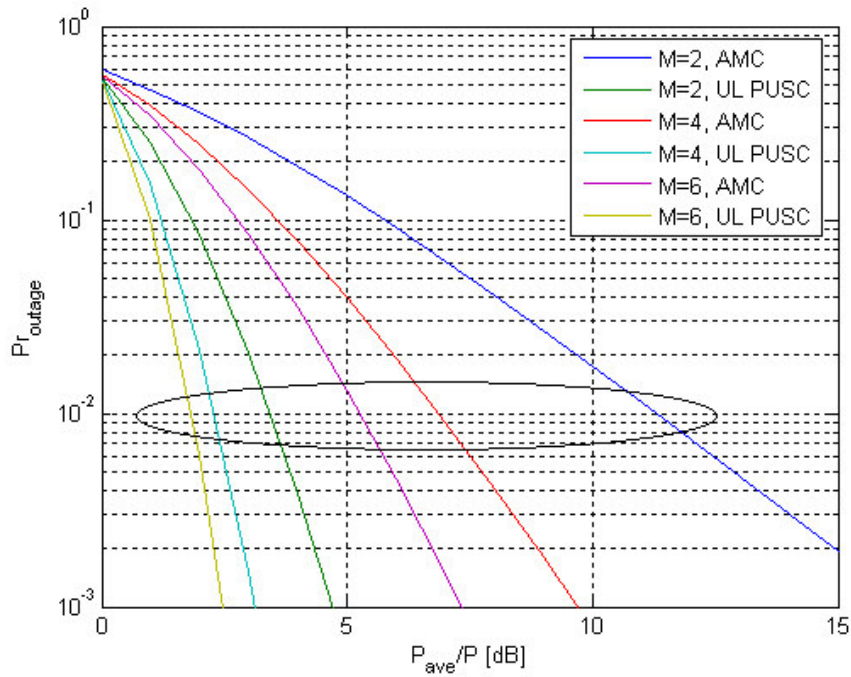


Figure 4 – Outage probability vs. fade margin. M is the number of antenna elements in the array.

The figure below shows the reduction of fade margin as a function of array size for the two permutations.

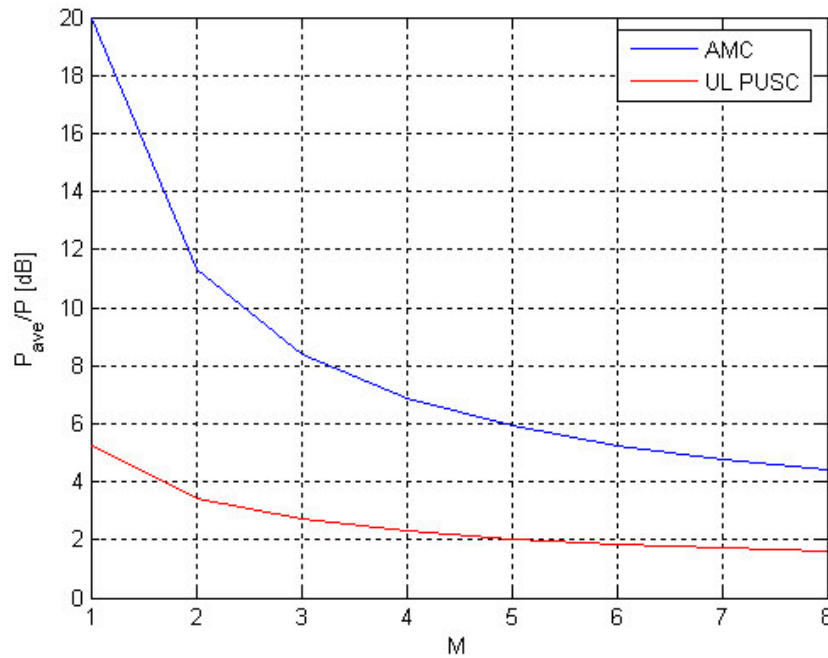


Figure 5 – Fade margin vs. number of antenna elements, for the both permutation

The fade margin of 4-4.5dB observed in the previous section is consistent with this analysis. It can be concluded that adding frequency diversity will have a positive impact on the system fade margin by an order of 4dB, in the close of 4-6 antenna elements.

3 Proposed Solution

We propose to add new permutation structures in the downlink called ‘Tile Usage of Sub-Channels’ (TUSC) and ‘Optional Tile Usage of Sub-channels’ (OTUSC). The properties of these permutations are similar to those of the uplink PUSC and OPUSC zones, except that segmentation and the subchannel rotation scheme are disabled.

In order to improve the channel tracking capabilities in spatial multiplexed transmissions, the tile’s pilots may be divided between SSs. This is achieved through extensions to the already defined physical modifier IEs and MIMO DL IEs.

4 Detailed Text Changes

1. [Modify section 8.4.3.1, page 498 lines 38-48 as follows]

----- BEGIN -----

- For downlink FUSC using the distributed subcarrier permutation (defined in 8.4.6.1.2.2 and 8.4.6.1.2.2.2), one slot is one subchannel by one OFDMA symbol.
- For downlink PUSC using the distributed subcarrier permutation (defined in 8.4.6.1.2.1), one slot is one subchannel by two OFDMA symbols.
- For uplink PUSC using either of the ~~distributed~~ distributed subcarrier permutations (defined in 8.4.6.2.1 and 8.4.6.2.5), and for downlink TUSC and optional TUSC (defined in sections 8.4.6.1.2.4 and 8.4.6.1.2.5), one slot is one subchannel by three OFDMA symbols.
- For uplink and downlink using the adjacent subcarrier permutation (defined in 8.4.6.3), one slot is one subchannel by one OFDMA symbol.

----- END -----

2. [Modify section 8.4.4.2, page 502 lines 48-52]

----- BEGIN -----

The OFDMA frame may include multiple zones (such as PUSC, FUSC, PUSC with all subchannels, optional FUSC, AMC, ~~and~~ optional FUSC with all subchannels, TUSC, and optional TUSC), the transition between zones is indicated in the DL-Map by the Zone_switch IE (see 8.4.5.3.4). No DL-MAP or UL-MAP allocations can span over multiple zones. Figure 219 depict OFDMA frame with multiple zones.

----- END -----

3. [Replace figure 219 on page 503 with the following figure]

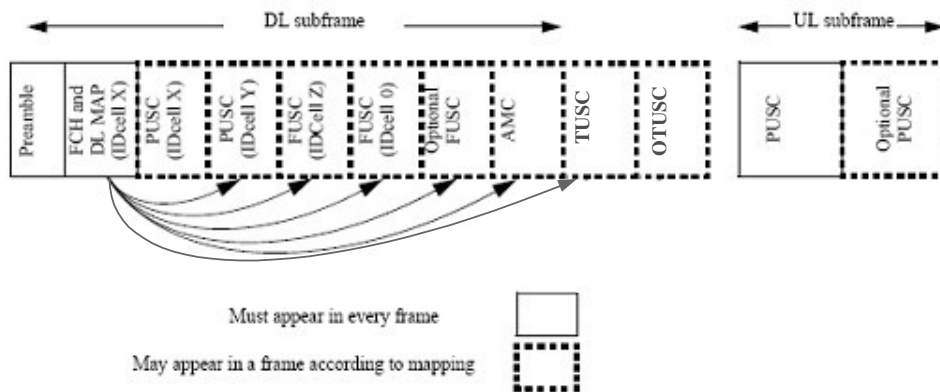


Figure 219 – Illustration of OFDMA frame with multiple zones

4. [Modify table 273 in section 8.4.5.3, starting from 'OFDMA Symbol Offset', as follows]

OFDMA Symbol offset	8 bits	
<u>If (Permutation = 0b11) and (Other Permutation select = AMC and AMC type is 2x3 or 1x6) or (Other Permutation select is TUSC or OTUSC)) {</u>		<u>In zones with TUSC / OTUSC permutation</u>
<u>{</u>		
<u>Subchannel offset</u>	<u>8 bits</u>	
<u>Boosting</u>	<u>3 bits</u>	<u>As defined below.</u>
<u>No. OFDMA triple symbols</u>	<u>5 bits</u>	<u>Number of OFDMA symbols is given in multiples of 3 symbols</u>
<u>No. Subchannels</u>	<u>6 bits</u>	
<u>}</u>		
<u>Else {</u>		
Subchannel offset	6 bits	
Boosting	3 bits	000: normal (not boosted); 001: +6dB; 010: -6dB; 011: +9dB; 100: +3dB; 101: -3dB; 110: -9dB; 111: - 12dB;.
No. OFDMA Symbols	7 bits	
No. Subchannels	6 bits	
<u>}</u>		

5. [Modify table 276 in section 8.4.5.3.3]

----- BEGIN -----

Table 276—OFDMA downlink AAS IE

Syntax	Size	Notes
AAS_DL_IE() {		
Extended DIUC	4 bits	AAS = 0x02
Length	4 bits	Length = 0x03
Permutation	2 bits	0b00 = PUSC permutation 0b01 = FUSC permutation 0b10 = Optional FUSC permutation 0b11 = adjacent-subcarrier permutation / other permutation (see 'other permutation select' field)
Preamble indication	2 bits	0b00 = No preamble 0b01 = Preamble used 0b10-0b11 = <i>Reserved</i>
First bin index	6 bits	When Permutation=0b10, this indicates the index of the first band allocated to this AMC segment
Last bin index	6 bits	When Permutation=0b10, this indicates the index of the last band allocated to this AMC segment
<u>If (length = 0x04) {</u>		
<u>Other permutation select</u>	<u>2 bits</u>	<u>0b00 = AMC</u> <u>0b01 = PUSC-ASCA</u> <u>0b10 = TUSC</u> <u>0b11 = OTUSC</u> <u>Applicable when Permutation = 0b11</u>
<u>Reserved</u>	<u>6 bits</u>	
<u>}</u>		
}		

----- END -----

6. [Modify table 277a in section 8.4.5.3.4]

----- BEGIN -----

Table 277a — OFDMA downlink TD_ZONE IE format

Syntax	Size	Notes
STC_ZONE_IE() {		
Extended DIUC	4	STC/ZONE = 0x01
Length	4	Length = 0x02
Permutation	2	00 = PUSC permutation 01 = FUSC permutation 10 = Optional FUSC permutation 11 = Optional adjacent subcarrier permutation / other permutation (see 'other permutation select' field)
Use All SC indicator	1	0 = Do not use all subchannels 1 = Use all subchannels
STC	2	0b00 = No transmit diversity 0b01 = STC using 3 antennas 0b10 = STC using 4 antennas 0b11 = FHDC using 2 antennas
Matrix Indicator	2	Antenna STC/FHDC matrix (see 8.4.8) 00 = Matrix A 01 = Matrix B 10 = Matrix C (applicable to 3 or 4 antennas only) 11 = reserved
IDcell	6	
Midamble presence	1	0 = not present 1 = present at the first symbol in STC zone
Midamble boosting	1	0 = no boost 1 = Boosting (3dB)
2/3 antennas select	1	0 = STC using 2 antennas 1 = STC using 3 antennas Selects 2/3 antennas when STC = 01
If (length = 0x03) {		
Dedicated Pilots	1	0 = Pilot symbols are broadcast 1 = Pilot Symbols are dedicated. An MSS should use only pilots specific to its burst for channel estimation
Other permutation select	<u>2</u>	0b00 = AMC 0b01 = PUSC-ASCA 0b10 = TUSC 0b11 = OTUSC Applicable when Permutation = 0b11
Reserved	7 <u>5</u>	
}		
}		

----- END -----

7. [Change 'Preamble Time Shift Index' entries in table 284 (section 8.4.5.3.11) as follows]

----- BEGIN -----

If (Time index shift type == 0) {		
Preamble Time Shift Index	4 bits	For PUSC, 0 – 0 sample cyclic shift

		<p>1 – floor($NFFT/14$) sample cyclic shift 13 – floor($NFFT/14*13$) sample cyclic shift 14-15 – reserved</p> <p>For AMC permutation, 0 – 0 sample cyclic shift 1 – floor($NFFT/9$) sample cyclic shift 8 – floor($NFFT/9*8$) sample cyclic shift 9-15 – reserved</p> <p><u>For TUSC permutation.</u> <u>0 – 0 sample cyclic shift</u> <u>1 – floor($NFFT/4$) sample cyclic shift</u> <u>2 – floor($NFFT/4*2$) sample cyclic shift</u> <u>3 – floor($NFFT/4*3$) sample cyclic shift</u> <u>4-15 – reserved</u></p> <p><u>For OTUSC permutation.</u> <u>0 – 0 sample cyclic shift</u> <u>1 – floor($NFFT/3$) sample cyclic shift</u> <u>2 – floor($NFFT/3*2$) sample cyclic shift</u> <u>3-15 – reserved</u></p>
} else {		
Preamble Time Shift Index	4 bits	<p>For PUSC, 0 – 0 sample cyclic shift 1 – floor($NFFT/14$) sample cyclic shift 13 – floor ($NFFT/14*13$) sample cyclic shift 14-15 – reserved</p> <p>For AMC permutation, 0 – 0 sample cyclic shift 1 – floor ($NFFT/9$) sample cyclic shift 8 – floor ($NFFT/9*8$) sample cyclic shift 9-15 – reserved</p> <p><u>For TUSC permutation.</u> <u>0 – 0 sample cyclic shift</u> <u>1 – ($NFFT/4$) sample cyclic shift</u> <u>2 – ($NFFT/4*2$) sample cyclic shift</u> <u>3 – ($NFFT/4*3$) sample cyclic shift</u> <u>4-15 – reserved</u></p> <p><u>For OTUSC permutation.</u> <u>0 – 0 sample cyclic shift</u> <u>1 – ($NFFT/3$) sample cyclic shift</u> <u>2 – ($NFFT/3*2$) sample cyclic shift</u> <u>3-15 – reserved</u></p>
}		

----- END -----

8. [Modify 8.4.5.4.14 lines 47-52, page 548]

----- BEGIN -----

The Physical Modifier Information Element indicates that the subsequent allocations shall utilize [a specific pilot pattern and](#) a preamble, which is either cyclically rotated in frequency or cyclically delayed (see Equation (100) and Equation (101)). [It further modifies the absolute starting slot of the next allocation.](#) The PHYMOD_UL_IE

can appear anywhere in the UL map, and it shall remain in effect until another PHYMOD_UL_IE is encountered, or until the end of the UL-map.

----- END -----

9. *[Modify table 300 (section 8.4.5.4.14) as follows]*

----- BEGIN -----

<u>Pilot pattern</u>	<u>2 bits</u>	<u>Pilot pattern to be used by subsequent allocations:</u> <u>0b00 = Use all pilots</u> <u>0b01 = Use pilot pattern A</u> <u>0b10 = Use pilot pattern B</u> <u>0b11 = reserved</u>
<u>Slot Offset</u>	<u>12 bits</u>	<u>In OFDMA slots (8.4.3.1)</u>
<i>reserved</i>	<u>53 bits</u>	

----- END -----

10. *[Add the following text before the end of section 8.4.5.4.14]*

----- BEGIN -----

Pilot pattern

The pilot pattern to be used in subsequent allocations. AAS-enabled SSS that do not support collaborative SM shall ignore this field and utilize all pilots.

Slot Offset

The offset of the slot in which the next allocation shall begin, relative to the start of the zone.

----- END -----

11. *[Add new sections 8.4.6.1.2.4, 8.4.6.1.2.4.1, 8.4.6.1.2.4.2]*

----- BEGIN -----

8.4.6.1.2.4 Optional downlink tile usage of subchannels (TUSC)

The optional downlink TUSC is similar in structure to the uplink PUSC structure defined in section 8.4.6.2. Each transmission uses 48 data subcarriers as the minimal block of processing. The permutation properties are given in tables 311, 311b-d.

The pilots in the TUSC permutation are regarded as part of the allocation, and as such shall be beamformed in a way that is consistent with the transmission of the allocation's data subcarriers

8.4.6.1.2.4.1 Symbol structure for TUSC subchannels

The TUSC symbol structure corresponds to that of the uplink PUSC structure as defined in section 8.4.6.2.1.

8.4.6.1.2.4.2 Partitioning of subcarriers into TUSC subchannels

The partitioning of subcarriers into tiles and tiles into subchannels corresponds to the definitions for the uplink PUSC structure as defined in section 8.4.6.2.2 with *UL IDcell* replaced by *IDcell*.

----- END -----

12. *[Add new sections 8.4.6.1.2.5, 8.4.6.1.2.5.1, 8.4.6.1.2.5.2]*

----- BEGIN -----

8.4.6.1.2.5 Additional Optional structure for TUSC (OTUSC)

The additional optional downlink TUSC (OTUSC) is similar in structure to the uplink optional PUSC structure defined in section 8.4.6.2.5. Each transmission uses 48 data subcarriers as the minimal block of processing. The permutation properties are given in tables 313, 313a-b.

The pilots in the TUSC permutation are regarded as part of the allocation, and as such shall be beamformed in a way that is consistent with the transmission of the allocation's data subcarriers

8.4.6.1.2.5.1 Symbol structure for OTUSC subchannels

The OTUSC symbol structure corresponds to that of the uplink optional PUSC structure as defined in section 8.4.6.2.5.1.

8.4.6.1.2.5.1 Partitioning of subcarriers into OTUSC subchannels

The partitioning of subcarriers into tiles and tiles into subchannels corresponds to the definitions for the uplink optional PUSC structure as defined in section 8.4.6.2.5.2.

----- END -----

13. [Modify 'Permutation' entry in table 311, section 8.4.6.2.7.1]

----- BEGIN -----

Permutation	<u>3</u> 2 bits	0b <u>0</u> 00 = PUSC perm. 0b <u>0</u> 01 = FUSC perm 0b <u>0</u> 10 = Optional FUSC perm. 0b <u>0</u> 11 = Adjacent subcarrier perm. <u>0b100 = PUSC-ASCA</u> <u>0b101 = TUSC</u> <u>0b110 = OTUSC</u> <u>0b111 = reserved</u>
--------------------	----------------------------	---

----- END -----

14. [Modify text in section 8.4.8.3, page 335 lines 3-10 as follows:]

Five ~~Three~~ optional zones for the downlink, the optional FUSC, optional AMC, ~~and the~~ optional PUSC-ASCA, optional TUSC and optional OTUSC zones, are described in 8.4.6.1.2.3, 8.4.6.3-~~and~~, 8.4.6.3.1, 8.4.6.1.2.4 and 8.4.6.1.2.5, respectively. STC may be used to improve system performance for these zones as well as for the mandatory PUSC zone and an example of transmit diversity (TD) with multiple transmitters and multiple receivers is shown in Figure 251a.

15. [Add new section 8.4.8.3.7]

----- BEGIN -----

8.4.8.3.7 Symbol structure for the TUSC and OTUSC permutations

Two STC modes for 2-antenna configuration are defined for the TUSC permutation. In both modes, the pilots in each tile shall be split between the two antennas as depicted in figure XXX. In the first mode, identified by STC matrix indicator 'A', data subcarriers are encoded within each tile after constellation mapping. In this mode, the

[files shall be allocated to subchannels and the data subcarriers enumerated as defined in 8.4.6.1.2.4. The data subcarriers transmitted from Antenna #0 follow the original mapping defined in 8.4.6.1.2.4.](#)

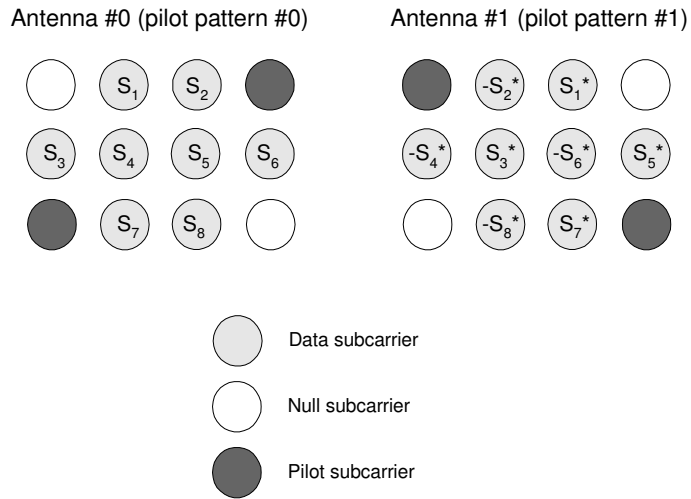


Figure XXX – Mapping of data subcarriers in STC for TUSC with matrix indicator A.

[The second STC mode for the TUSC permutation provides spatial multiplexing and is identified by the following matrix \(row index indicates antenna number, column index indicates slot duration\):](#)

$$\underline{B} = \begin{matrix} \underline{S}_1 \\ \underline{S}_2 \end{matrix} \quad (\text{AAA})$$

[The STC modes for the OTUSC permutation correspond to the definitions for the uplink optional PUSC as defined in sections 8.4.8.4.1-3, with pilot pattern A regarded as pilot pattern #0, and pattern B regarded as pilot pattern #1.](#)

----- END -----

16. *[Modify section 8.4.9.4.3, page 620 lines 54-57]*

----- BEGIN -----

For the mandatory tile structure in the uplink, [and for the TUSC structure in the downlink in non-STC modes](#), pilot subcarriers shall be inserted into each data burst in order to constitute the symbol and they shall be modulated according to their subcarrier location within the OFDMA symbol.

----- END -----

17. *[Modify section 8.4.9.4.3, page 621 lines 1-3]*

----- BEGIN -----

In the downlink, [except for the TUSC structure](#), and for the optional uplink tile structure each pilot shall be transmitted with a boosting of 2.5 dB over the average power of each data tone. The Pilot subcarriers shall be modulated according to the following formula:

----- END -----

18. *[Add the following text before the end of section 8.4.9.4.3]*

----- BEGIN -----

[For the TUSC structure in STC mode, the pilots shall be boosted such that the total power per pilot in each tile is equal to the total pilot power in the non-STC mode.](#)

----- END -----

19. *[Modify table in section 11.8.3.7.5]*

----- BEGIN -----

Type	Length	Value	Scope
154	1	Bit# 0: Optional PUSC support Bit# 1: Optional FUSC support Bit# 2: AMC support Bit# 3: TUSC support Bit# 4: OTUSC support Bits# 3 5-7: Reserved, shall be set to zero	SBC-REQ (see 6.3.2.3.23) SBC-RSP (see 6.3.2.3.24)

----- END -----

5 Acknowledgement

The authors would like to acknowledge Dr. Jack Cohen for his assistance in preparing the analysis and simulation in section 2.1.

6 References

- [1] R. B. Ertel, P. Cardieri, K. W. Sowerby, T. S. Rappaport and J. H. Reed, "*Overview of Spatial Channel Models for Antenna Array Communication Systems*", IEEE Personal Communications • February 1998 pp 10-22,
- [2] J. Fuhl, A. F. Molisch, and E. Bonek, "Unified channel model for mobile radio systems with smart antennas," IEE Proc. Radar, Sonar, Navig., vol. 145, pp. 32–41, Feb. 1998.
- [3] C. Ward, M. Smith, A. Jeffries, D. Adams, and J. Hudson, "Characterizing radio propagation channel for smart antenna systems," Electron. Commun. Eng. J., pp. 191–201, Aug. 1996.
- [4] R. Janaswamy, "Angle and Time of Arrival Statistics for the Gaussian Scatter density Model" IEEE TRANSACTIONS ON WIRELESS COMMUNICATIONS, VOL. 1, NO. 3, JULY 2002, pp 488-497
- [5] K. I. Pedersen, P. E. Mogensen, and B. H. Fleury, , "A stochastic model of the temporal and azimuthal dispersion seen at the base station in outdoor propagation environments," IEEE Trans. Veh. Technol., vol. 49, pp. 437–447, Mar. 2000.
- [6] IEEE P802.16-2004.